International Journal of Concrete Structures and Materials

RESEARCH Open Access

Applicability of Core–Shell Hybridization Approach Using Natural and Recycled Aggregate Concrete

Ji-Hyun Kim[1], Andres Salas-Montoya[2], Young-Chan Kim[1] and Chul-Woo Chung[1*]

Abstract

The aim of this research is to propose a novel technique to improve the performance of structural concrete member using recycled aggregate by creating a core–shell hybrid concrete instead of intermixing natural aggregate concrete with recycled aggregate concrete. The technique involves layered casting of a recycled aggregate concrete with natural aggregate concrete, either as a core or as a shell, to prove whether this core–shell hybridization approach has a potential to facilitate the utilization of recycled aggregate for structural concrete. Various core–shell combinations were made using w/c 0.3 and 0.5 concretes, and compressive strength, elastic modulus, and chloride ion diffusivity of the hybrid specimens were measured. This paper also investigated the effects of two-stage mixing approach on properties of recycled aggregate concrete and hybrid concrete. It was found that placing stronger NAC at the outer shell provided higher compressive strength and elastic modulus of core–shell hybrid concrete. Placing NAC at the outer shell also provided lower chloride ion diffusivity as it acted as a diffusion barrier. It is recommended to place a stronger and more durable natural aggregate concrete in the shell to have better mechanical properties and durability. A synergetic effect of hybridization was observed from elastic modulus, not from the compressive strength. It was also found that compressive strength and elastic modulus of core–shell hybrid concrete were successfully estimated using those of control concrete specimens.

Keywords Recycled aggregate, Layered casting, Two-stage mixing, Compressive strength, Elastic modulus, Core–shell hybrid

1 Introduction

The global search for new aggregates due to the critical shortage of natural resources has led to the exploration of recycled materials as an alternative to replace natural aggregates (NA) to address aggregate demand, environmental concerns, and production costs (Alawais & West, 2019; Beiser, 2019; Fiorato, 1989; Hama et al., 2023; Kawai, 2005; Mehta et al., 1991; Tam & Tam, 2007). The use of recycled aggregates (RA) is an urgent issue in Republic of Korea due to its limited land capacity and higher disposal cost (Kim, 2021; Makul et al., 2021). Despite the growing interest in sustainability, the widespread use of recycled aggregate concrete (RAC) for structural applications has been quite limited (Kim, 2021; González-Fonteboa et al., 2018; Shaban et al., 2019a; Tam et al., 2018; Zheng et al., 2021; Alyaseen et al., 2023a, 2023b; Lipczynska et al., 2021) because RA generally exhibits inferior performance than NA. The reason is associated with weak interfacial transition zone, porous and transverse cracking, durability-related cracking, high impurities, poor grading, etc., all of which

Journal information: ISSN 1976-0485 / eISSN 2234-1315.

*Correspondence:
Chul-Woo Chung
cwchung@pknu.ac.kr
[1] Division of Architectural and Fire Protection Engineering, Pukyong National University, Yongso-Ro 45, Nam-Gu, Busan 48513, Republic of Korea
[2] Department of Civil Engineering, Universidad Nacional de Colombia, Carrera 27 # 64-60, Manizales, Caldas, Colombia

cause variability in aggregate quality (Butler et al., 2013; González-Fonteboa et al., 2018; González-Taboada et al., 2016; Katz, 2004; Li et al., 2009). These characteristics have a significant impact on various concrete properties, including density, modulus of elasticity, compressive, flexural, tensile, split tensile and bond strengths, as well as shrinkage (Faysal et al., 2020; Silva et al., 2018). Extensive test results from different researchers have shown that the properties of RAC tend to show more variability compared to natural aggregate concretes (NAC) (González-Fonteboa et al., 2018; Singh et al., 2020; Tam et al., 2018; Yehia et al., 2015). Therefore, to utilize RA that requires high quality control, it is critical to address these limitations. The difficulty of ensuring a consistent level of quality in RAC has resulted in a cautious approach by governmental policies towards its broad implementation.

For the successful implementation of RA, further research is needed to understand the properties, cost–benefit, and performance of RAC (Beiser, 2019; Kawai, 2005; Richard, 1984; Salas et al., 2013; Salas_Montoya et al., 2023). To achieve equal or comparable performance to NAC, researchers have proposed various techniques to mitigate the adverse effects caused by RA (Butler et al., 2013; Li et al., 2009; Liang et al., 2015; Ouyang et al., 2020; Silva et al., 2018; Tam et al., 2023; Zhang et al., 2018). Among the most cited, three approaches could be highlighted: (a) the removal of old mortar from RA using chemical, mechanical, or thermal methods (Butler et al., 2013; Faysal et al., 2020; Katz, 2004; Kisku et al., 2017; Li et al., 2009; Liang et al., 2015; Mistri et al., 2022; Ouyang et al., 2020; Shaban et al., 2019a, 2019b, 2021; Tam & Tam, 2007; Tam et al., 2021, 2023; Xuan et al., 2016; Zhang et al., 2018; Zheng et al., 2021), (b) strengthening the old mortar in RA by filling cracks and micropores through surface coatings, solution immersion, or chemical reactions and (c) improvements of concrete mix design process (Ouyang et al., 2020; Tam et al., 2021; Xuan et al., 2016; Zhang et al., 2018; Zheng et al., 2021). Each technique offers specific advantages while facing certain limitations (Shaban et al., 2021; Zheng et al., 2021). Although the first two approaches can provide high quality RA, they also generate additional waste solutions that require high disposal cost. However, the third approach only requires a small change in the mixing procedure without significant modification in production facility. Therefore, the two-stage mixing approach (TSMA) (Kisku et al., 2017; Liang et al., 2015; Shaban et al., 2019b, 2021; Tam & Tam, 2007; Tam et al., 2006, 2018; Xuan et al., 2016; Zheng et al., 2021) became one of the most widely accepted approaches to improve the properties of RAC.

TSMA, introduced by Tam et al. (Tam et al., 2021), modifies the conventional concrete mixing process to achieve superior mechanical performance of RAC, particularly for structural applications (Brand et al., 2015; Salas et al., 2013; Salas-Montoya & Mira-Rada, 2023). The TSMA involves a change in the mixing sequence where a portion of the cementitious materials and water are first combined with the RA to form a cement slurry. This slurry efficiently adheres to the RA, resulting in compaction of the interfacial transition zone between the RA and the cement paste (Faysal et al., 2020). In addition, TSMA facilitates the healing of cracks present in the old interfacial transition zone and in the RA. In the second stage of TSMA, the remaining materials are added to the mixer to produce RAC (Tam & Tam, 2008; Tam et al., 2006). This method has shown promising results in improving the mechanical properties of RAC, significantly improving their compressive strength, making it a potential solution for obtaining high quality RAC for various construction purposes (Faysal et al., 2020; Salas_Montoya et al., 2023), with improvement of compressive strength up to 21% observed for a replacement of mixing approach (Tam & Tam, 2008; Tam et al., 2018, 2023). The only disadvantage of TSMA is that the additional (separated) mixing procedure may require a bit more of attention from the operator.

Although TSMA improved the mechanical properties of RAC and opened the way for more sustainable and effective use of RA, further research is needed to explore more variables such as the production of special concretes to optimize RAC performance (Faysal et al., 2020; Salas_Montoya et al., 2023; Shaban et al., 2019a). Some additional momentum that can ignite the widespread use of RA is crucial to address the urgent adoption of RA as a substitute for NA. To advance this goal, this work presents a novel approach to improve the performance of structural concrete member made of RAC. A layered construction of NAC and RAC to make a core–shell hybrid concrete by optimizing its distribution within the cross-section of structural elements, is proposed. Previous studies have shown successful applications of such combination by incorporating high strength or ultra-high strength concrete as an outer shell to provide a confinement effect (Mander et al., 1988; Ronanki & Aaleti, 2022; Wu, 2019). Since the results from previous works have shown a potential applicability of utilizing core–shell hybrid concrete, this work focuses on the application of a layered casting technique of NAC and RAC in the vertical direction to expand the applicability of RAC.

This is the first experimental work investigating the compressive strength, elastic modulus, and chloride ion diffusivity of such hybrid concretes. Strength and

modulus were measured to represent the mechanical performance under compression, and chloride ion diffusivity was measured to investigate the effect of different core–shell combination on potential corrosion resistance of hybrid concrete. The preparation of RAC was carried out using both the normal mixing approach and the TSMA. In this context, the term "hybrid" is preferred over "composite" because it specifically denotes the layered casting of RAC and NAC. The use of the term "composite" could cause confusion or misunderstanding, as it also refers to materials containing fibers and a resin matrix.

2 Experimental Procedure

2.1 Materials

Type I ordinary portland cement (Ssangyong Cement, Co. Ltd., Seoul, Republic of Korea) was used to prepare concrete specimens. The chemical compositions of the portland cement are shown in Table 1. A natural fine aggregate produced in Jumunjin, Republic of Korea, with a bulk specific density of 2.58 g/cm^3, a fineness modulus 2.41, and an absorption capacity of 1.87%, was used for all concrete mixes. The chemical compositions of the aggregates are also presented in Table 1. Two sources of coarse aggregate were used: crushed stone (NA) and RA. The crushed stone has a nominal maximum size of 20 mm, bulk specific density of 2.70 g/cm^3, and fineness modulus of 6.60. RA has a nominal maximum size of 13 mm, a bulk specific density of 2.34 g/cm^3 and a fineness modulus of 6.22. The absorption capacity of NA and RA were 1.23% and 3.43%, respectively. Polycarboxylate ester type high range water reducer (The One Chemical Korea INC.) was used to obtain sufficient workability. Mineral admixture and air entraining agent were not used.

2.2 Mix Proportions

Eighteen concrete mix designs were formulated and produced using NA and RA with two different water/cement ratios: 0.3 to produce high strength concrete and 0.5 to produce conventional strength concrete. Three different types of concretes, NAC, RAC, and RAC mixed by TSMA, were prepared at each w/c. The amount of the individual constituents used in each concrete mix is shown in Tables 2 and 3. Volumes of aggregates were kept constant between the mixes, and, in RAC, 100% of coarse aggregate was composed of RA. Coarse and fine aggregates were mixed to adjust the gradation to the limits recommended by ASTM C33 (ASTM International, 2018) to produce workable and compactable concrete mixes. Polycarboxylate based high range water reducer was used at different dosages by weight of cement to obtain similar workability levels (target slump value of 100 ± 20 mm) for each concrete.

2.3 Mix Procedures

As noted above, two different mixing methods, normal mixing and TSMA, were used to produce the concrete mixes. Normal mixing followed the guidelines of ASTM C192 (ASTM International & ASTM C192, 2019). For normal mixing, coarse and fine aggregates in a saturated surface dry state were placed in a pan mixer together with portland cement. Dry mixing was performed for 30

Table 1 Chemical compositions of materials used in this work

Materials		CaO	Fe_2O_3	SiO_2	MgO	Al_2O_3	MnO	P_2O_5	TiO_2	SO_3
OPC		63.42	3.04	19.48	3.11	4.69	0.13	0.2	0.38	4.08
Fine Aggregate		1.24	1.65	74.71	1.03	13.21	–	0.08	0.3	0.06
Coarse Aggregate	Natural	8.93	7.01	52.85	3.64	19.29	0.17	0.54	1.02	0.28
	Recycled	15.94	2.46	57.20	2.37	15.30	–	0.22	0.49	0.35

Table 2 Mix proportions of control concrete specimen

Control Specimen	w/c	Amount of material (kg/m^3)					
		Water	Cement	Aggregate			SP* (%)
				Fine	Natural crushed	Recycled	
Natural crushed aggregate concrete (N3)	0.3	158.87	529.56	694.55	1090.29	–	0.313
Recycled aggregate concrete (R3)	0.3	158.87	529.56	694.55	–	944.91	0.349
Natural crushed aggregate concrete (N5)	0.5	200	400	694.55	1090.29	–	–
Recycled aggregate concrete (R5)	0.5	200	400	694.55	–	944.91	–

* Written as weight percent of cement

Table 3 Identification of 4 mix designs to make 18 distinct fabrication conditions for core–shell hybrid concrete specimens

Type	Specimen	Details of specific specimen			
		Aggregate type (volume ratio, %)		W/C	Two-stage mixing approach (TSMA)
		Shell part	Core part		
Control	N3	Natural crushed (100)		0.3	–
	R3	Recycled (100)			–
	R_T3	Recycled (100)			○
	N5	Natural crushed (100)		0.5	–
	R5	Recycled (100)			–
	R_T5	Recycled (100)			○
Hybrid	R3N3	Recycled (75)	Natural crushed (25)	0.3	–
	N3R3	Natural crushed (75)	Recycled (25)		–
	R_T3N3	Recycled (75)	Natural crushed (25)		○
	$N3R_T3$	Natural crushed (75)	Recycled (25)		○
	R5N5	Recycled (75)	Natural crushed (25)	0.5	–
	N5R5	Natural crushed (75)	Recycled (25)		–
	R_T5N5	Recycled (75)	Natural crushed (25)		○
	$N5R_T5$	Natural crushed (75)	Recycled (25)		○
	R3N5	Recycled (75)	Natural crushed (25)	0.3 & 0.5	–
	N3R5	Natural crushed (75)	Recycled (25)		–
	R_T3N5	Recycled (75)	Natural crushed (25)		○
	$N3R_T5$	Natural crushed (75)	Recycled (25)		○

* The letter N for natural aggregate, NA, R for RA, and subscript T for TSMA with RA. For example, "$N3R_T5$" indicates NAC of w/c 0.3 was placed on the outside (shell) and RAC of w/c 0.5 mixed with TSMA (subscripted) was placed in the core of the specimen. The number written in the parenthesis by the aggregate designation, e.g., Recycled (75), indicates the volume fraction of concrete made of such specific aggregate (RA)

s, and mixing water was added. Fresh concrete was mixed at 30 rpm for 30 s and 60 rpm for 1 min.

TSMA was performed according to a modified version proposed by the authors (Kim et al., 2020; Park et al., 2022). The coarse and fine aggregates were placed in the pan mixer in a saturated surface dry (SSD) condition and subjected to a dry mixing process for 30 s. Simultaneously, type I ordinary portland cement and mixing water were individually combined using a commercial planetary paddle mixer according to the guidelines of the ASTM C 305 (ASTM international & ASTM C305, 2011). Upon completion of the cement paste mixing, the prepared cement paste was poured into the pan mixer. The concrete was mixed at 30 rpm for 30 s, followed by mixing at 60 rpm for 1 min.

2.4 Casting and Curing

Immediately after mixing, slump test was performed on control concrete specimens according to ASTM C 143 (ASTM International, 2020) to measure the workability. For the concrete which met the target slump of 100 ± 20 mm, layered casting of core–shell hybrid concretes in cylinders of 100 mm × 200 mm was performed using plastic core formwork shown in Fig. 1a. The formwork was designed to maintain the concentricity of two concretes as accurately as possible.

After mixing, fresh concrete was placed into the shell (outer) part of the cylinder, compacted, and vibrated to remove entrapped air. Photographic image after completion of shell casting is shown in Fig. 1b. The core (center) part of the concrete was cast about 5 to 10 min after casting of the shell part, as shown in Fig. 1c. After concrete in the cylinders was completely filled, the plastic formwork that separated core and shell part of the concrete was slowly removed to avoid the void inclusion at the interface between core and shell (Fig. 1d). In fact, concretes placed on both core and the shell were slightly overfilled because the level of concrete sank down after removal of the plastic formwork. After removal of the plastic formwork (Fig. 1e), top of concrete specimen was screed to make a flat surface. The top of the specimen after completion of layered casting is shown in Fig. 1f. As note from Fig. 1f, top surface of freshly cast concrete did not show clear difference from that of normal concrete specimen.

After casting, the concrete specimens were covered, sealed with plastic wrap, and stored in the laboratory under controlled temperature (20 ± 2 °C) for 24 h to maintain initial moisture conditions. The specimens were

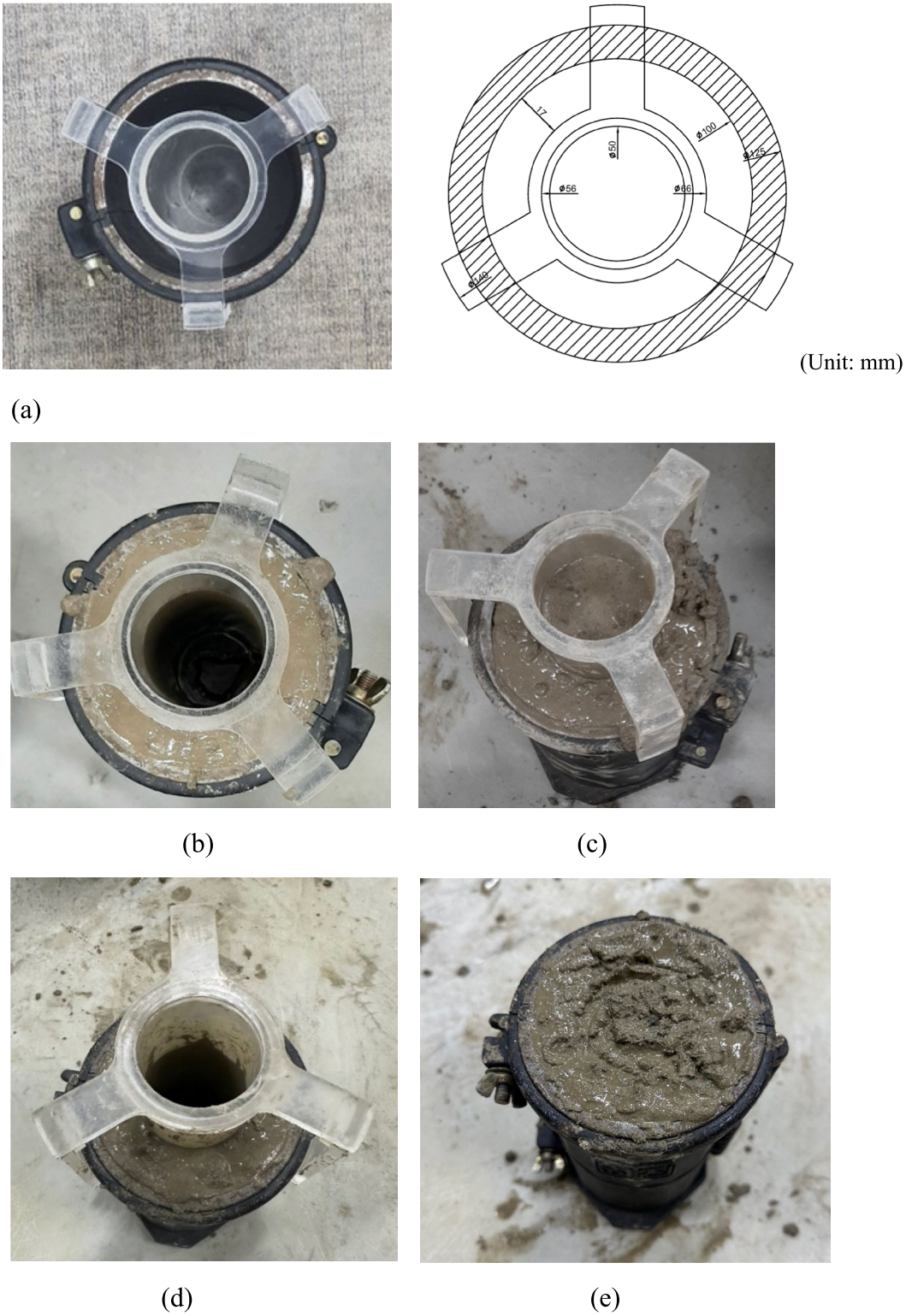

Fig. 1 Layered casting of core–shell hybrid concrete: **a** plastic core formwork, **b** after completion of casting shell part, **c** after completion of casting core part, **d** removal of plastic formwork, **e** after completion of formwork removal, and **f** after completion of screeding the surface of fresh core–shell hybrid concrete

(f)

Fig. 1 continued

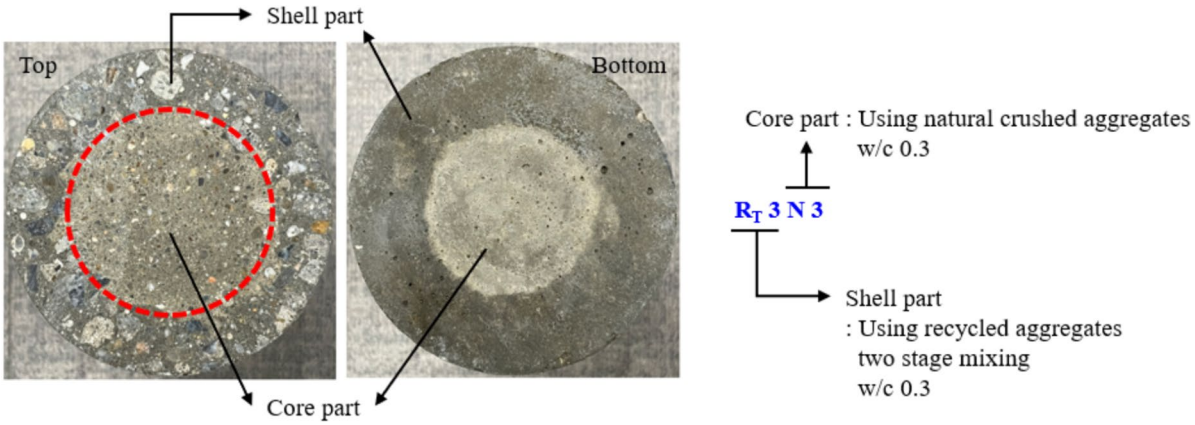

Fig. 2 Photographic images on the surface of core–shell hybrid concrete (R_T3N3 specimen) with a designation used for identification of core–shell hybrid concrete specimens. Note that not all concrete showed such a distinct difference between core and shell. The constituent of top part was visible due to the surface grinding of the specimen for compression test

then demolded and immersed in a saturated lime solution at 20 ± 2 °C until 180-day. A photographic images showing the surface of hardened core–shell hybrid concrete are presented in Fig. 2. It should be noted that such a well-developed distinction between core and shell was one of the extreme cases. All other core–shell hybrid concrete showed similar shape but less identifiable compared with case shown in Fig. 2.

2.5 Compressive Strength and Elastic Modulus

Tests were conducted according to ASTM standard test procedures to determine the compressive strength and elastic modulus of hardened concrete. At 180 days, a compressometer was first fixed at the center part of the 100 mm × 200 mm cylindrical concrete specimen, two linear variable displacement transducers (LVDT; CDP-10, Tokyo Measuring Instruments Lab, Tokyo, Japan) were installed to a compressometer (Tokyo Measuring Instruments Lab, Tokyo, Japan), and the testing specimen was placed on top of the 1,000 kN load cell, as shown in Fig. 3a. The load cell and LVDTs were connected to a static datalogger (TDS 530, Tokyo Measuring Instruments Laboratory Co. ltd., Japan), shown in Fig. 3b, to collect the data during measurement.

Three test specimens were used for the measurements of compressive strength and elastic modulus. During the measurement, loading rate was maintained at 0.25 MPa/s as specified at ASTM C 39 (ASTM International &

(a) (b)

Fig. 3 Photographic images of compressive strength and elastic modulus measurement test set-up: **a** with load cell and compressometer and (**b**) whole testing setup with the data logger

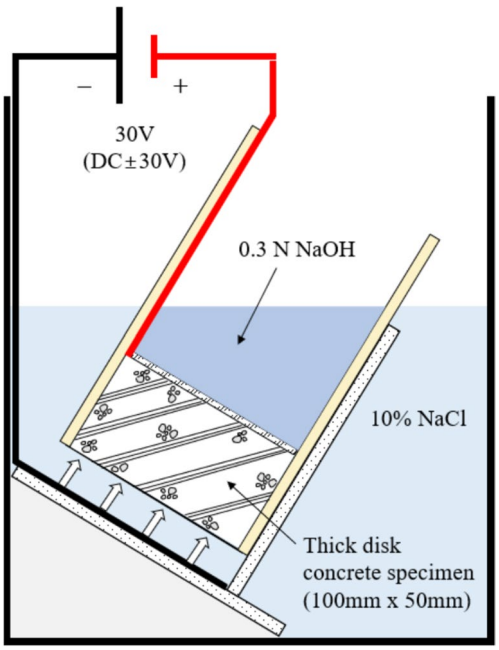

Fig. 4 Schematic illustration of test set-up used for NT Build 492 test procedure

ASTM C39, 2021) and ASTM C 469 (ASTM international & ASTM C469, 2010). Peak load was used to obtain compressive strength, and elastic modulus was calculated using following equation:

$$E = (S_2 - S_1)/(\varepsilon_2 - 0.00005) \quad (1)$$

where E is chord modulus (MPa), S_2 is 40% of the maximum stress, S_1 is the stress at strain rate of 0.00005, ε_2 is the strain that corresponds to 40% of the maximum stress, respectively.

2.6 Chloride Ion Penetration

The resistance to chloride ion penetrability was determined using Rapid Chloride Permeability Test Apparatus (PROOVE`it, Germann Instruments, Denmark) according to NT-Build 492 (Nordtest, 1999) at 180 days of curing using a portion of the cylinders. Cylindrical concrete specimens were cut into 50 mm thick disk specimens (100 mm × 50 mm), placed in a testing cell shown in Fig. 4. The 0.3 N NaOH solution was placed into the anode (on top of specimen) and 10% NaCl solution was poured into the cathode (outside container). A 30 V (DC ± 30 V) voltage was applied to the cell and the initial current amount was measured, and voltage for testing was determined as specified in NT-Build 492 (Nordtest, 1999). The test was conducted for a total of 24 h after the initial measurement process were completed.

3 Test Results and Analyses

3.1 Overall Behavior and Failure Mode of Test Specimens

Most specimens, both control or core–shell hybrid concretes, failed due to crushing. In case of core–shell hybrid concrete specimens, it was difficult to identify a clear fracture line along the NAC and RAC interface as shown in Fig. 5. Very rarely, shear failure pattern was observed across the interface as shown in Fig. 5c. This unexpected pattern might be resulted from the stronger core part (N5) which acted as a wedge to the weaker shell part (R5), thereby leading to a shear failure. In Fig. 5c, d, f, it can be found that fracture lines were extended seamlessly through the cross section without interruption at the interface. As found in Fig. 5, the unintentionally produced indentation of interface caused by the interlocking of the aggregate was observed, which became a reason for improvement of bonding between NAC and RAC. This result suggests that with sufficient curing time and strict quality control of the RAC, a monolithic behavior can be expected at the interface of NAC and RAC.

3.2 Compressive Strength

Fig. 6 shows the compressive strength of specimens with series 3 and 5 (w/c of 0.3 and 0.5, respectively). When comparing control concrete specimens of R3 and R5 to NAC (N3 and N5), their compressive strengths were inferior by 16.0% and 6.1%, respectively. This was expected as the use of RA reduces compressive strength of concrete. However, for R_T3 and R_T5 (with the case of two-stage mixing), the reduction in compressive strength was less for 6.6% and 2.4%, respectively. The results agreed well with what was observed from the works of Tam et al. (Tam & Tam, 2008; Tam et al., 2006, 2018, 2021), which showed higher strength with TSMA than normal

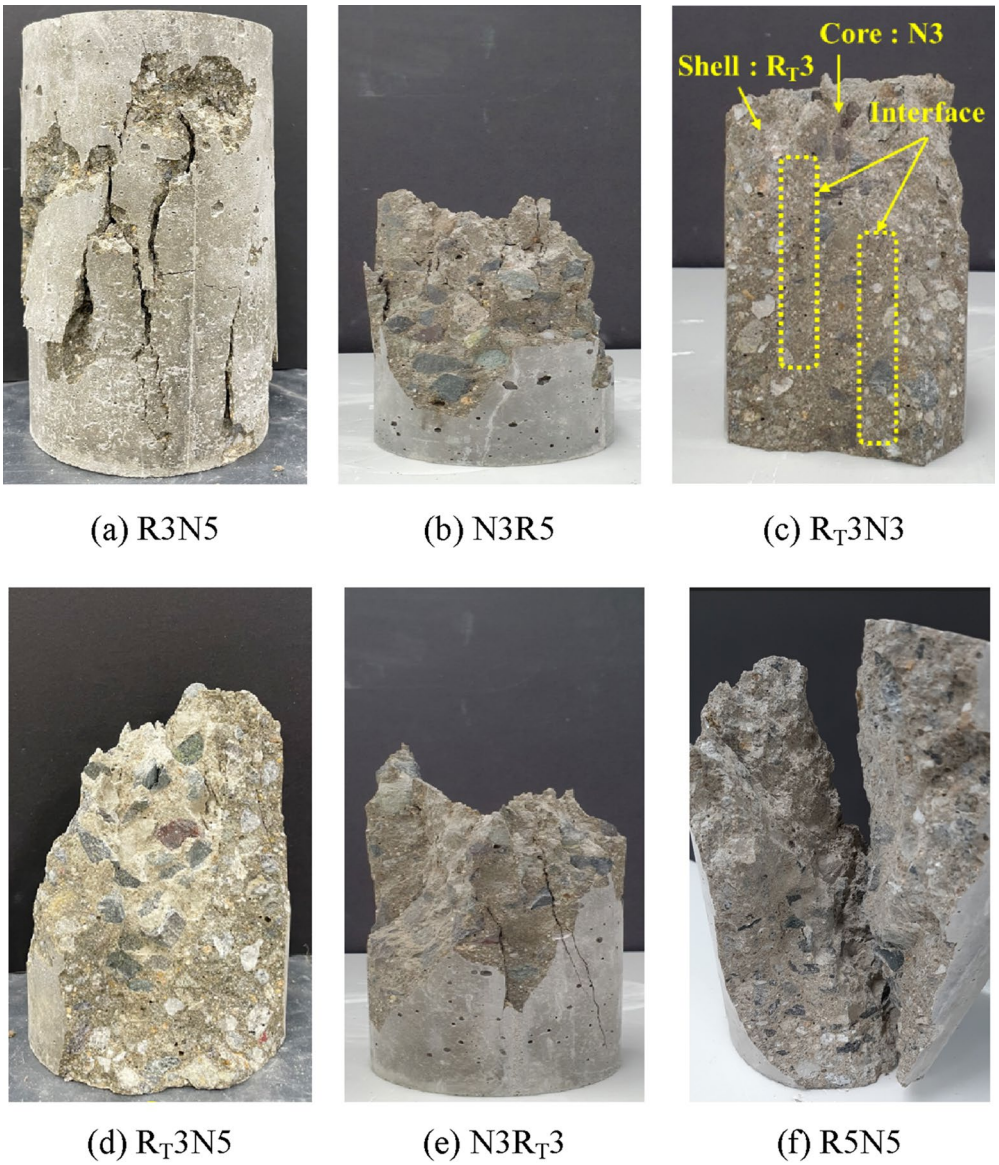

Fig. 5 Photographic images of concrete after compression test

mixing approach, suggesting that improved consistency in strength was obtained by TSMA due to stable interaction between concrete components.

In Series 3 (with w/c 0.3), specimens of R3N3 and R_T3N3 had lower compressive strength compared to the other specimens. This means stronger NAC placement at the outer shell is more beneficial for the core–shell hybrid approach. However, in Series 5, specimens of R5N5 and R_T5N5 did not show a significant variation in compressive strength compared to the other specimens. The compressive strength of N5RT5 and RT5N5 was also almost identical to each other. These results suggest that the beneficial effect caused by the placement of NAC at outer shell (from w/c 0.3 concrete) became less effective when w/c was increased to w/c 0.5.

The data presented in Table 4 show the percentage of increase in compressive strength between Series 5 (data from Fig. 6b) and Series 3 (data from Fig. 6a). This analysis also showed that w/c ratio significantly affected the compressive strength of the control concrete specimens containing N or R_T, as well as the core–shell hybrid concrete specimens with N on the outer shell.

Fig. 7 shows the compressive strength of the core–shell hybrid concrete specimens made of different w/c concrete. It is noteworthy that when N3 was placed on the outer shell, there was no significant difference between

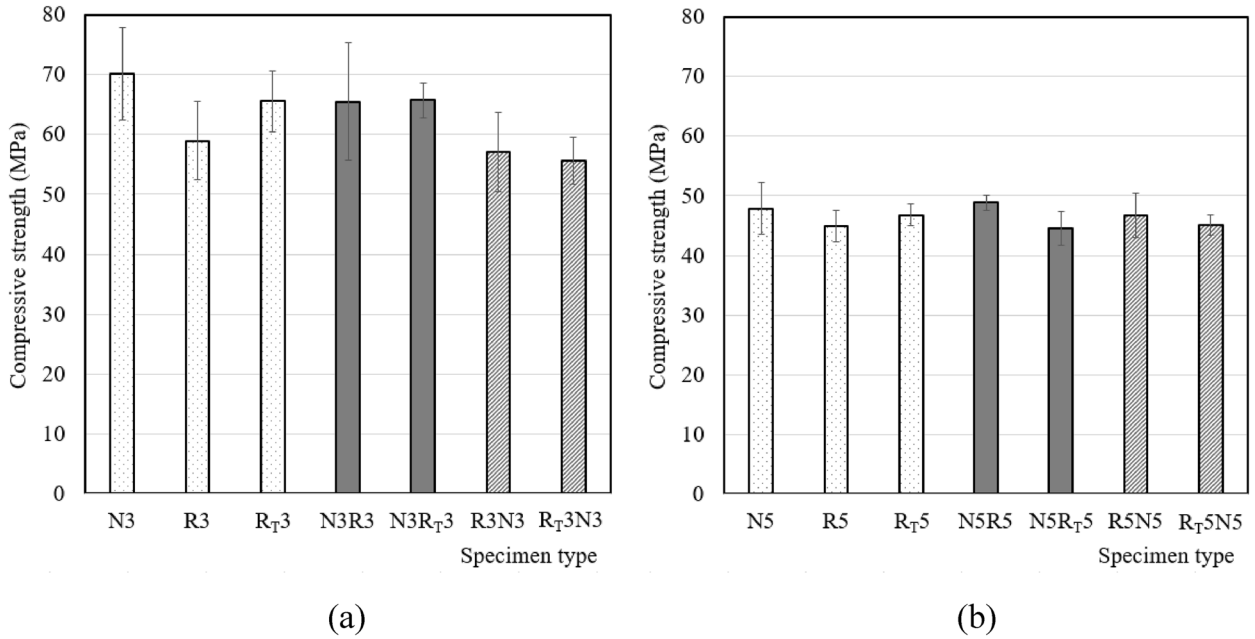

Fig. 6 Compressive strength of series 3 (w/c of 0.3) and 5 (w/c of 0.5) concrete specimen: **a** series 3 and (**b**) series 5

Table 4 Percent increase in compressive strength from series 5 to series 3 specimen

Specimen	N	R	R_T	NR	NR_T	RN	R_TN
Increase (%)	46.47	31.10	40.16	33.93	47.50	22.22	23.50

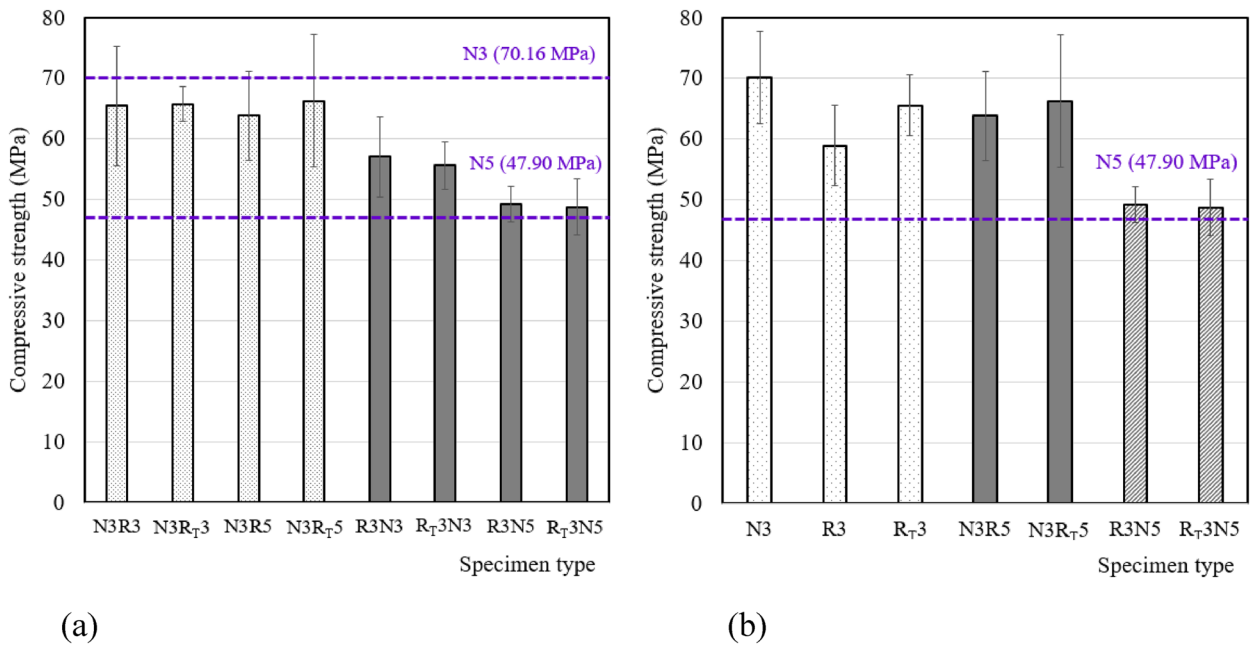

Fig. 7 Compressive strength of core–shell hybrid concrete specimen: **a** effect of NAC and RAC placement and **b** effect of series combination. Note that purple dotted lines in the figure were compressive strengths of N3 and N5 concrete, respectively

the specimens regardless of the type of inner core concrete (as shown in Fig. 7a). This result could be attributed to the larger surface area (75%) of the outer shell (NAC) and the confinement effect caused by the NAC, which has higher strength than RAC, thereby resulting in almost no reduction in compressive strength. When different w/c ratios were used to produce the core–shell hybrid concrete, N3R5 and N3R_T5 showed a reduction in compressive strength of 9.0% and 5.5%, respectively, compared to N3. In contrast, R3N5 and R_T3N5 exhibited compressive strengths similar to N5, although the compressive strength of N5 was significantly lower than that of R3 and R_T3 (as shown in Fig. 7b). These results indicate that the placement of NAC on the outer shell is more preferable for optimizing the performance of core–shell hybrid concrete.

3.3 Elastic Modulus

Fig. 8 shows elastic modulus of Series 3 (w/c 0.3) and 5 (w/c 0.5) concretes. The elastic moduli of control concrete specimens of R3 and R5 were lower than those of NAC (N3 and N5) by 3.8% and 7.9%, respectively. However, elastic modulus of R_T3 and R_T5 was higher than that of NAC by 0.5% and 7.9%, respectively. It is interesting to note that the core–shell hybrid concrete specimen with NAC in the outer shell showed a higher performance than control concrete specimen of NAC in terms of elastic modulus. The reason can also be attributed to the stronger outer core (NAC) had higher surface area to maximize the confinement effect and to increase resistance by interlocking of aggregate at the interface of NAC and RAC as observed from Fig. 5.

The effect of w/c ratio on elastic modulus was less pronounced compared to its effect on compressive strength. As shown in Table 5, which presents the percentage increase in elastic modulus between Series 5 (data from Fig. 8b) and Series 3 (data from Fig. 8a), the maximum increase was 22.32% for the R specimen. In general, the percentage increase in elastic modulus was much smaller compared to the case of compressive strength, where the N-R_T specimen showed a 47.50% increase in compressive strength.

The elastic moduli of the core–shell hybrid concrete specimens with N3 on the outer shell showed similarities regardless of the type of inner core concrete (as shown in Fig. 9a), consistent with the trend observed for compressive strength. An interesting observation was made regarding the elastic modulus of N3R5 and N3R_T5.

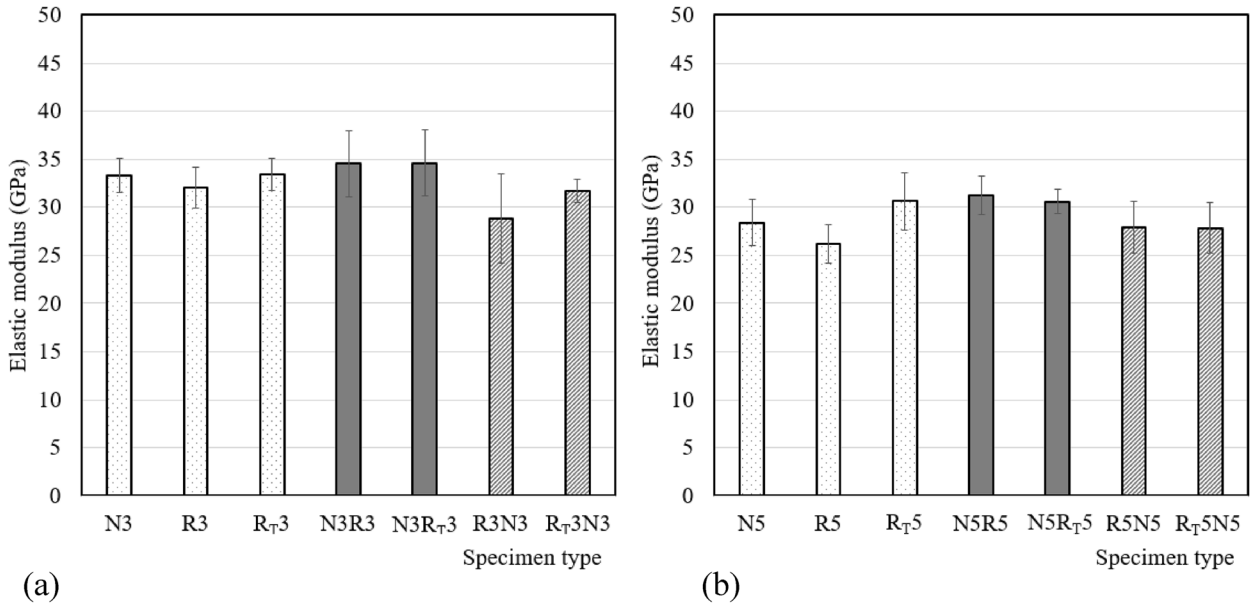

Fig. 8 Elastic modulus of series 3 (w/c of 0.3) and 5 (w/c of 0.5) concrete specimen: **a** series 3 and **b** series 5

Table 5 Percent increase in elastic modulus from series 5 to series 3 specimen

Specimen	N	R	R_T	NR	NR_T	RN	R_TN
Increase (%)	17.11	22.32	9.12	10.53	13.07	3.25	13.81

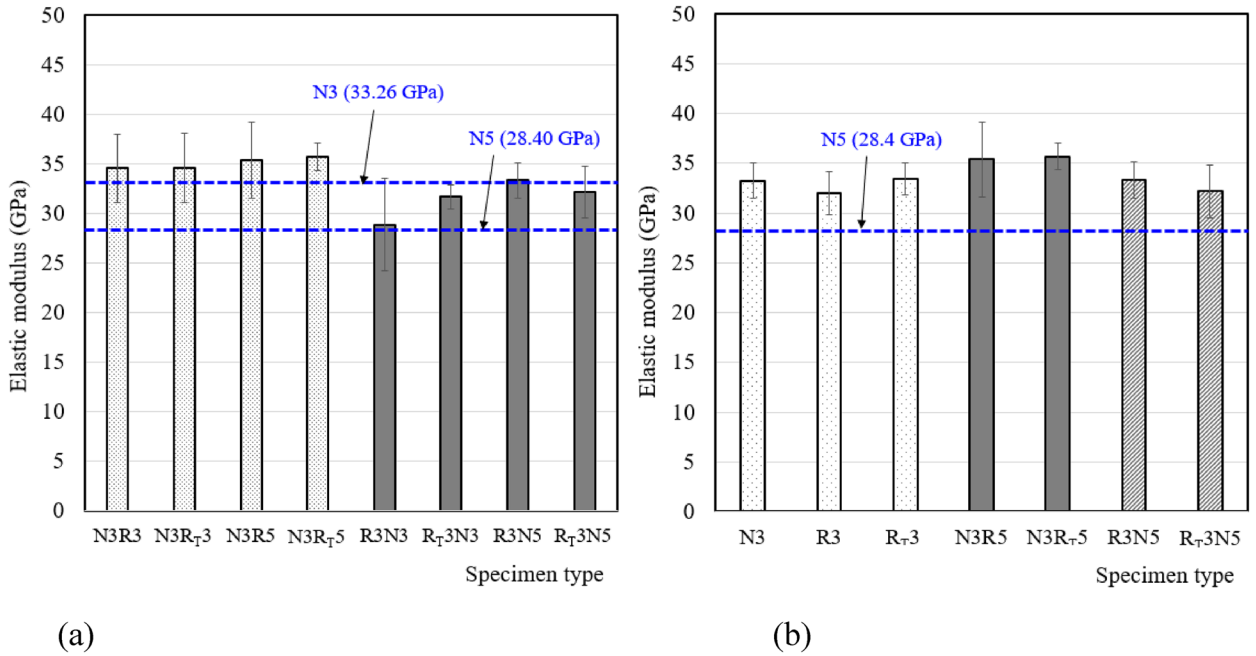

Fig. 9 Elastic modulus of core–shell hybrid concrete specimen: **a** effect of NAC and RAC placement and **b** effect of series combination. Note that purple dotted lines in the figure were elastic moduli of N3 and N5 concrete, respectively

Since R3 is stronger than R5 and R_T5, elastic modulus was expected to be lower than that of N3R3. However, contrary to the expectation, the opposite results were observed. It was because concrete with higher elastic modulus acted as a strain inhibitor to increase dimensional stability of core–shell hybrid concrete, thereby causing a synergetic effect in elastic modulus. The synergetic effect seemed to be more evident in the case of R3N5 and R_T3N5 (as shown in Fig. 9a), but it was also possible that the location of the core was slightly shifted during casting of core–shell specimens. In such case, the case of R3N3 can be better considered as an experimental outlier (caused by shifting of core location) since elastic modulus is more susceptible to loading direction (location of core and shell) than compressive strength.

In addition, elastic modulus for N3R5 and N3R_T5 was slightly higher than that of N3, which contrasted with the behavior observed for compressive strength. The elastic modulus for R3N5 and R_T3N5 was similar to that of R3 and R_T3, respectively, while their compressive strength was similar to that of N5 (as shown in Fig. 9b). These results reveal interesting differences between elastic modulus and compressive strength in core–shell hybrid concrete specimens with N3 on the outer shell. At this moment, the interlocking effect caused by different sized coarse aggregate (NA for 20 mm and RA for 13 mm) is considered as one of the reasons. Further research is necessary to fully understand such synergetic effect.

3.4 Estimation on Compressive Strength and Elastic Modulus of Core–Shell Hybrid Concrete

An analytical calculation was used to estimate the compressive strength and elastic modulus of core–shell hybrid concrete specimens using the compressive strength and elastic modulus data of control concrete specimens (NAC and RAC only concretes). Since the compressive strains within the cores are consistent, the following Eq. (2) is established:

$$\varepsilon = \frac{P_i}{E_i A_i} = \frac{P_o}{E_o A_o} = \frac{P}{E_h A} \tag{2}$$

, where E, A, and P represent the elastic modulus, the loading area of the specimen, and the applied load, respectively. The subscripts *i, o,* and *h* correspond to the inner core, outer shell, and hybrid section, respectively. If inner core was RAC, E_i became elastic modulus of control RAC concrete (RAC only), and if inner core was NAC, E_i became elastic modulus of control NAC concrete. The same rule applied for all other cases. It is worth noting that the area of the outer shell (A_o) is three times larger than that of the inner core (A_i), A becomes equal to $4A_i$. Since the load applied to the core–shell hybrid concrete specimen can be expressed by Eq. (3), the compressive strength of the core–shell hybrid concrete can be determined by dividing the applied load by the cross-sectional area of the specimen and using the ratio of strains in the inner core and outer shell as shown in Eq. (4):

$$P = P_i + P_o \tag{3}$$

$$\sigma_h = \frac{P}{A} = \frac{(1+\frac{E_i}{3E_o})P_o}{\frac{4}{3}A_o} = \frac{3E_o+E_i}{4E_o}\sigma_o \tag{4}$$

Similar analytical approach shown in the compressive strength estimation of core–shell hybrid specimens was followed to estimate the elastic modulus of core–shell hybrid concrete specimens. Using Eqs. (2) and (3), the following relation can be established as the Eq. (5).

$$\frac{P_o}{E_oA_o} = \frac{P}{E_hA}, P_i = \frac{E_i}{3E_o}P_o \tag{5}$$

From Eq. (5), elastic modulus of the core–shell hybrid concrete specimen can be calculated as Eq. (6).

$$E_h = \frac{E_i + 3E_o}{4} \tag{6}$$

Fig. 10 illustrates the discrepancy between the measured compressive strength and elastic modulus of the core–shell hybrid concrete and the estimated properties derived from the values obtained from the control NAC and RAC concrete specimens. Equations (4) and (6) were used to estimate the compressive strength and elastic modulus of the core–shell hybrid concrete, respectively.

Based on the data shown in Fig. 10a, there was a strong correlation between the measured and estimated compressive strength values. Among the core–shell hybrid concrete specimens, R_T3N3 and R3N5 showed differences of more than 10%. In general, the estimated compressive strength tended to be slightly higher than the measured compressive strength, but the measured values still showed a remarkable agreement with the estimated values.

For elastic modulus, three core–shell hybrid concrete specimens, N5R5, N3R5, and R3N3, showed differences greater than 10% (Fig. 10b). Interestingly, unlike the compressive strength scenario, the measured elastic modulus was higher than the estimated elastic modulus. The deviations from the line of equality for the elastic modulus were more dispersed than those observed for the compressive strength; however, the measured elastic modulus consistently showed a solid correlation with the estimated elastic modulus. These results indicate that the compressive strength and elastic modulus of core–shell hybrid concrete can be effectively estimated using data obtained from control concrete specimens.

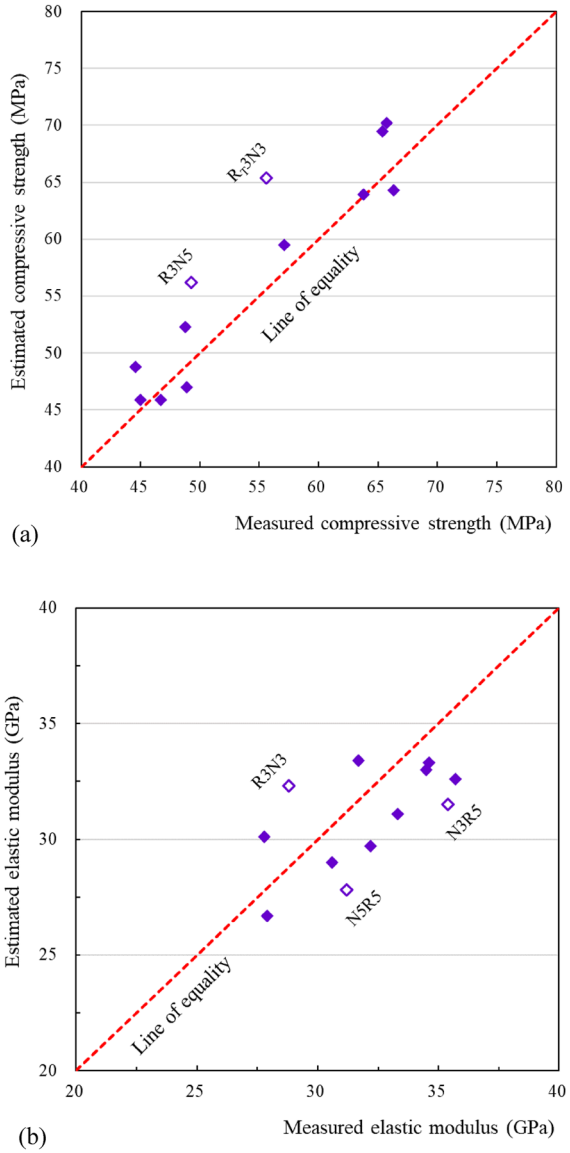

Fig. 10 Comparison between measured mechanical and estimated values of core–shell hybrid concrete: **a** measured compressive strength vs. estimated compressive strength and **b** measured elastic modulus vs. estimated elastic modulus

3.5 Chloride Ion Penetration

The core–shell hybrid concrete specimens were subjected to the NT-BUILD 492 test method (Nordtest, 1999) to measure their chloride ion diffusivity. Fig. 11 shows the chloride ion diffusivity of the Series 3 and 5 concretes. The test results indicate that the NA mixes had much lower chloride ion diffusivity than the RA mixes for both series. The control samples, N3 and N5 showed chloride ion diffusivity of 1×10^{-12}m^2/s and 3.8×10^{-12}m^2/s after 180 days of curing, respectively. The effect caused by TSMA was not clearly identified in terms of chloride ion diffusivity. In case of core–shell hybrid concrete, chloride ion diffusivity ranged between that of NAC and RAC. This is mainly because

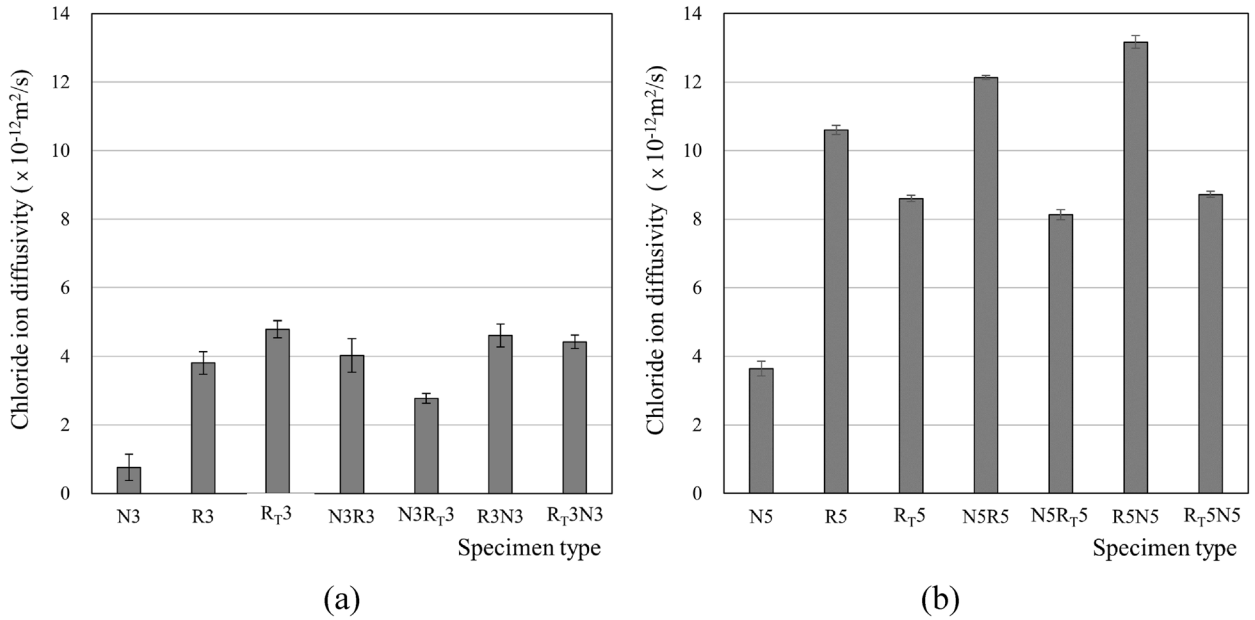

Fig. 11 Chloride ion diffusivity of series 3 (w/c of 0.3) and 5 (w/c of 0.5) concrete specimen: **a** Series 3 and **b** Series 5

RAC had a more porous structure at the aggregate—cement paste interface than NA concretes as mentioned by Poon et al. (Poon et al., 2004) and Kong et al. (Kong et al., 2010) which induced higher penetration of chloride ion through its matrix.

Fig. 12 shows the diffusivity of chloride ions measured from the core–shell hybrid concrete specimens. The use of different w/c ratios during the casting of the core–shell hybrid concrete resulted in an increase in chloride ion diffusivity compared to the use of the same w/c concrete for casting. Photographs in Fig. 13 illustrate the depth of chloride penetration in various core–shell hybrid concrete specimens. The photographs of the specimens showed a similar trend as the results presented in Figs. 11

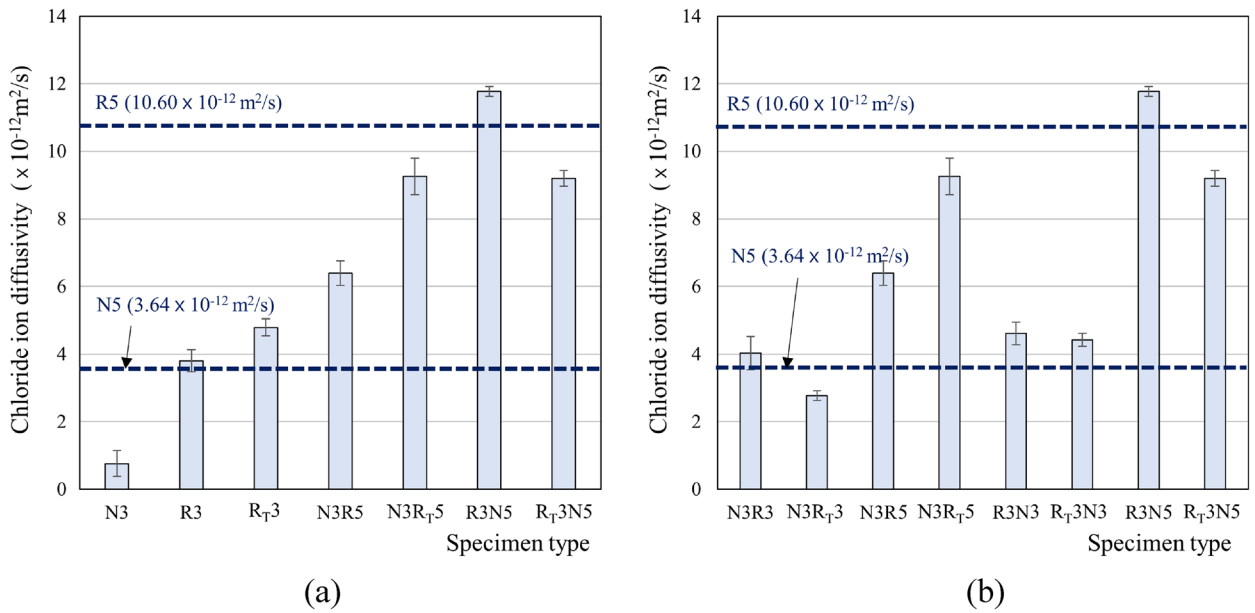

Fig. 12 Chloride ion diffusivity of core–shell hybrid concrete specimen: **a** effect of NAC and RAC placement and **b** effect of series combination. Note that blue dotted lines in the figure were chloride ion diffusivities of N5 and R5 concrete, respectively

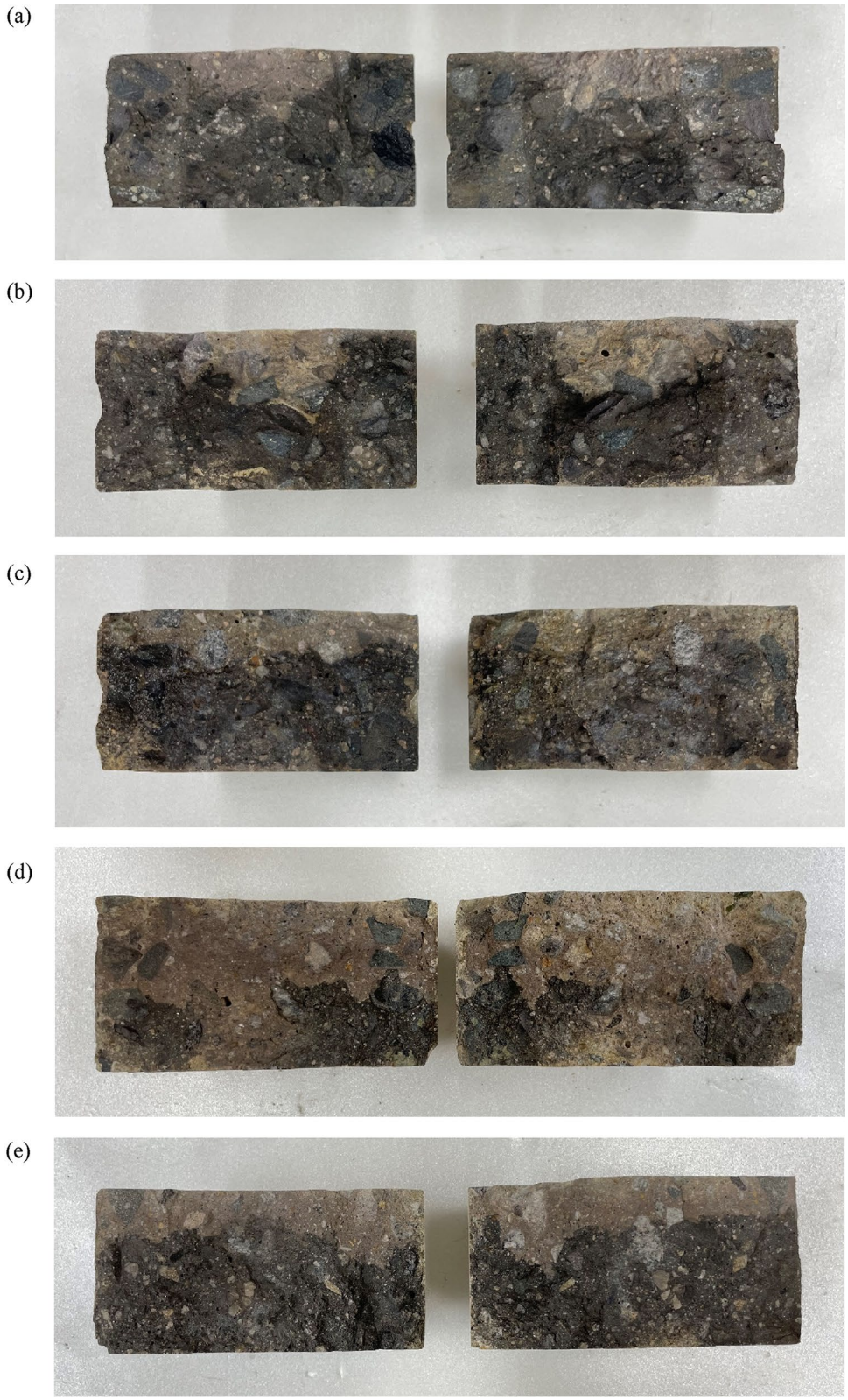

Fig. 13 Photographs of core–shell hybrid concrete after completion of the NT-BUILD 492 test procedure [59]: **a** N3R_T5 and **b** R3N5 for hybridization with the same w/c concretes and **c** N3R3 and **d** N5R5 for hybridization with different w/c concretes. **e** control specimen made of R_T3 without core–shell hybridization

and 12. Casting the core–shell hybrid concrete with different w/c ratios resulted in deeper chloride penetration depths (Fig. 13 (a) and (b)) in areas with higher w/c ratios (middle portion). Conversely, when the same w/c ratio was used (Fig. 13c and d), the difference in penetration depth was less pronounced. Therefore, for effective use of core–shell hybrid concrete, it is imperative that the shell portion of the concrete should be made of a stronger and more durable material, which is NAC. This robust concrete component would serve as an outer layer capable of bearing loads, causing a confinement effect, providing a diffusion barrier of aggressive ions, and ultimately prolonging the service life of the structure.

4 Discussion

This study examined the compressive strength, elastic modulus, and chloride ion diffusivity of core–shell hybrid concretes made of 18 different combinations with RAC and NAC. Considering the inherent values of RAC along with the effect of TSMA, the ranking of specimen performance can be established in the following descending order: (1) N, (2) N-R_T, (3) N-R, (4) R_T, and (5) R. Initially, improvements in compressive strength and elastic modulus were expected due to the reinforcing or confining effect caused by stronger concrete, particularly for core–shell hybrid specimens with a lower w/c. However, the experimental results did not consistently agree with this expected ranking. This can be found from R3, R_T3, and R_T5 specimens whose compressive strengths and elastic moduli were higher than those of R3N3, R_T3N3, R_T5N5, respectively, in which the reverse was physically expected. One of possible reasons for such behavior is the inherent difficulty in maintaining consistent compaction of concrete into narrow core and shell of hybrid specimen whose shell to core area ratio was 3. In this work, the thickness ratio of the inner to outer core was not varied to derive an affirmative conclusion on the roles or effects of core and shell. Further work using larger sized specimens (e.g., 150 mm × 300 mm cylindrical specimens or larger) needs to be performed to investigate the effect caused by various core to shell area (volume) proportions.

In this study, 100% RA was used to produce RAC concrete. An analytical approach was developed to estimate compressive strength and elastic modulus of core–shell hybrid concrete based on control concrete data, using theoretically driven equation. The result showed a strong correlation between estimated and measured compressive strengths and elastic moduli (Fig. 10). Overall, this study suggests that core–shell hybrid concrete properties can be estimated using data from control (NAC and RAC only) concrete specimens.

According to the experimental results, compressive strengths of all core–shell hybrid concretes were in the range of N3 (the highest strength) to R5 (the lowest compressive strength). When estimating the compressive strength of core–shell hybrid concrete based on the strength of the control concrete, the estimated strengths were slightly higher than the measured strengths. No synergetic effect seemed to be observed by use of core–shell specimen. However, some core–shell hybrid concretes (when N3 was used as a shell) exceeded the elastic modulus of N3 (the highest elastic modulus). Similarly, N5R5 and N5R_T5 showed higher elastic moduli than N5. When comparing estimated elastic moduli with measured moduli, the measured moduli were higher than estimated ones. All the results indicate that a synergetic effect in elastic modulus has been generated by the use of core–shell hybrid concrete. The causes of such synergetic effect in elastic modulus can be various, including that the confinement effect is more significantly working on elastic modulus than compressive strength. This confinement effect can be considered similar to the phenomenon that aggregate acts as a strain inhibitor to increase dimensional stability of concrete. Other reason can be attributed to the aggregate interlocking caused by different sized aggregate at the interface. However, nothing is clear at this moment. Given the limited scope of this study, factors such as core area ratio, shell thickness, specimen shape, and size need to be further investigated to better understand such effect.

It should be noted that there was no problem at the interface between RAC and NAC (core and shell). It was because there was no construction joint in the core–shell hybrid concrete. The core part of the concrete was cast within 10 min after casting the shell part of the concrete. Moreover, there was no clear indication on abrupt failure of the specimen related to the loss in compressive strength or in elastic modulus. If there was a problem at the interface, core–shell hybrid concrete should have presented much lower strength than the estimated value. The measured value had a strong correlation with the estimated one, and especially for elastic modulus, measured values were higher than estimated values which can be the evidence for a synergetic effect.

In this work, compressive strength and elastic modulus under compression was investigated. It was because the original intention of the core–shell hybridization approach was mainly targeted for the precast concrete because core–shell hybrid approach utilized in this work can only be applicable for the column. However, this core–shell hybrid approach can also be expanded to the layered placement of fresh concrete (RAC and NAC) at construction site. In construction site, two different pumping lines can

be installed to supply two different types of concretes (NAC and RAC) in sequence. In this case, it is not exactly "the core–shell approach" but is "the layered placement" that is similar to core–shell placement of fresh concrete that eliminates the construction joint. RAC can be placed where lower stress is expected, and NAC can be placed where higher stress is expected. To achieve such an objective, some additional tasks need to be conducted, for example measuring flexural strength of layered concrete made of NAC and RAC. Since properties such as split tensile and shear behavior are as equally important, such properties will need to be evaluated as the future works.

Finally, as noted from Fig. 13, some core–shell hybrid concretes, whose w/c of core and shell were different, had deeper chloride ion penetration compared to the control specimen (Fig. 13a, b, d). It was associated with higher chloride ion diffusivity of RAC that was located in the core. From the evaluation of compressive strength and elastic modulus as well as chloride ion diffusivity, a confinement effect (an enveloping effect in case of durability) is very important to enhance the performance of core–shell hybrid concrete. For successful application of core–shell hybrid concrete, it is critical to locate a stronger and more durable concrete, NAC, on the shell.

5 Conclusions

In this experimental investigation, a series of tests were conducted on core–shell hybrid concrete specimens that included compressive strength, elastic modulus, and chloride ion penetration measurements. The RCA replacement rate was maintained at 100% in the core or shell concrete. The effects of different concrete arrangements within the core and shell regions were investigated. The main findings of this study are as follows.

(1) The interface between NAC and RAC showed minimal evidence of segregation, meaning that the effective integration and strong bonding between the different types of concrete can be achieved.
(2) Specimens with R or R_T (RA with TSMA) in the outer core had lower compressive strength and elastic modulus than specimens with a single core of R or R_T. This suggests that placing NAC in the outer core position would give better results.
(3) Through the evaluation of the chloride ion diffusivities of core–shell hybrid concrete specimens, it is obvious that placing NAC in the shell would enhances the durability of the core–shell hybrid concrete.
(4) The predictions of compressive strength and elastic modulus for the core–shell hybrid using control concrete specimens were reasonably close to engineering accuracy.

Acknowledgements
This research was supported by the National Research Foundation (NRF) funded by the Korean government (MSIT) (No. RS-2024-00450130). Authors appreciate the assistance provided by Mr. Seung-Uk Heo and Jeong-Jin Son on preparation of materials and experiments.

Author contributions
Prof. Ji-Hyun Kim: Writing—Original Draft, Writing—Review & Editing, Formal analysis, conceptualization, Investigation, Methodology. Prof. Andres Salas-Montoya: Writing—Original Draft, Writing—Review & Editing, Conceptualization, Methodology. Prof. Young-Chan Kim: Writing—Review & Editing, Conceptualization, Methodology, Project administration, Formal analysis. Prof. Chul-Woo Chung: Writing—Review & Editing, Project administration, Conceptualization, Methodology, Formal analysis.

Funding
National Research Foundation of Korea (NRF) funded by the Korea government(Ministry of Science and ICT)(No. RS-2024–00450130).

Availability of data and materials
The datasets used and/or analyzed during the current study are available from the corresponding author on reasonable request.

Declarations

Competing interests
The authors declare that they have no competing interests.

Received: 3 September 2024 Accepted: 28 March 2025
Published online: 01 July 2025

References

Alawais, A., & West, R. P. (2019). Ultra-violet and chemical treatment of crumb rubber aggregate in a sustainable concrete mix. *Journal of Structural Integrity and Maintenance, 4*(3), 144–152. https://doi.org/10.1080/24705314.2019.1594603

Alyaseen, A., Poddar, A., Alahmad, H., Kumar, N., & Sihag, P. (2023a). High-performance self-compacting concrete with recycled coarse aggregate: Comprehensive systematic review on mix design parameters. *Journal of Structural Integrity and Maintenance, 8*(3), 161–178. https://doi.org/10.1080/24705314.2023.2211850

Alyaseen, A., Poddar, A., Kumar, N., Tajjour, S., Prasad, C. V. S. R., Alahmad, H., & Sihag, P. (2023b). High-performance self-compacting concrete with recycled coarse aggregate: Soft-computing analysis of compressive strength. *Journal of Building Engineering, 77*, 107527. https://doi.org/10.1016/j.jobe.2023.107527

ASTM International ASTM C469. 2010 Standard test method for static modulus elasticity and poissons ratio of concrete in compression. ASTM international.

ASTM International, ASTM C305, Standard practice for mechanical mixing of hydraulic cement paste and mortars of plastic consistency, ASTM international. 2011.

ASTM International, ASTM C33/C33M, Standard specification for concrete aggregates, ASTM International, West Conshohocken, 2018.

ASTM International, ASTM C192, Standard practice for making and curing concrete test specimens in the laboratory, ASTM International, West Conshohocken, 2019.

ASTM International, ASTM C143, Standard test method for slump of hydraulic-cement concrete, ASTM International. 2020.

ASTM International ASTM C39, Standard test method for compressive strength of cylindrical concrete specomens. ASTM international. 2021.

Beiser V., Why the world is running out of sand, BBC Future. 18 (8) (2019) https://www.bbc.com/future/article/20191108-why-the-world-is-running-out-of-sand.

Brand, A. S., Roesler, J. R., & Salas, A. (2015). Initial moisture and mixing effects on higher quality recycled coarse aggregate concrete. *Construction and Building Materials, 79*, 83–89. https://doi.org/10.1016/j.conbuildmat.2015.01.047

Butler, L., West, J. S., & Tighe, S. L. (2013). Effect of recycled concrete coarse aggregate from multiple sources on the hardened properties of concrete with equivalent compressive strength. *Construction and Building Materials, 47*, 1292–1301. https://doi.org/10.1016/j.conbuildmat.2013.05.074

Faysal, RMd., Maslehuddin, M., Shameem, M., Ahmad, S., & Adekunle, S. K. (2020). Effect of mineral additives and two-stage mixing on the performance of recycled aggregate concrete. *Journal of Material Cycles and Waste Management, 22*(5), 1587–1601. https://doi.org/10.1007/s10163-020-01048-9

Fiorato, A. (1989). PCA research on high-strength concrete. *Concrete International, 11*(4), 44–50.

González-Fonteboa, B., Seara-Paz, S., De Brito, J., González-Taboada, I., Martínez-Abella, F., & Vasco-Silva, R. (2018). Recycled concrete with coarse recycled aggregate An overview and analysis. *Materiales De Construcción, 68*(330), e151. https://doi.org/10.3989/mc.2018.13317

González-Taboada, I., González-Fonteboa, B., Martínez-Abella, F., & Carro-López, D. (2016). Study of recycled concrete aggregate quality and its relationship with recycled concrete compressive strength using database analysis. *Materiales De Construcción, 66*(323), e089. https://doi.org/10.3989/mc.2016.06415

Hama, S. M., Ali, Z. M., Zayan, H. S., & Mahmoud, A. S. (2023). Structural behavior of reinforced concrete incorporating glass waste as coarse aggregate. *Journal of Structural Integrity and Maintenance, 8*(1), 59–66. https://doi.org/10.1080/24705314.2023.2165470

Katz, A. (2004). Treatments for the improvement of recycled aggregate. *Journal of Materials in Civil Engineering, 16*(6), 597–603. https://doi.org/10.1061/(ASCE)0899-1561(2004)16:6(597)

Kawai T., State-of-the-art report on high-strength concrete in Japan-Recent developments and spplications. JSCE/VIFCEA Joint Seminar on Concrete Engineering. (2005) 87–107.

Kim, J. (2021). Construction and demolition waste management in Korea: Recycled aggregate and its application. *Clean Technologies and Environmental Policy, 23*(8), 2223–2234. https://doi.org/10.1007/s10098-021-02177-x

Kim, Y. J., Kim, G. W., & Chung, C. W. (2020). Contribution of two-stage mixing approach on compressive strength of mortar made of recycled fine aggregate. *Journal of the Korean Recycled Construction Resources Institute, 8*(4), 490–497. https://doi.org/10.14190/JRCR.2020.8.4.490

Kisku, N., Joshi, H., Ansari, M., Panda, S. K., Nayak, S., & Dutta, S. C. (2017). A critical review and assessment for usage of recycled aggregate as sustainable construction material. *Construction and Building Materials, 131*, 721–740. https://doi.org/10.1016/j.conbuildmat.2016.11.029

Kong, D., Lei, T., Zheng, J., Ma, C., Jiang, J., & Jiang, J. (2010). Effect and mechanism of surface-coating pozzalanics materials around aggregate on properties and ITZ microstructure of recycled aggregate concrete. *Construction and Building Materials, 24*(5), 701–708. https://doi.org/10.1016/j.conbuildmat.2009.10.038

Li, J., Xiao, H., & Zhou, Y. (2009). Influence of coating recycled aggregate surface with pozzolanic powder on properties of recycled aggregate concrete. *Construction and Building Materials, 23*(3), 1287–1291. https://doi.org/10.1016/j.conbuildmat.2008.07.019

Liang, Y., Ye, Z., Vernerey, F., & Xi, Y. (2015). Development of processing methods to improve strength of concrete with 100% recycled coarse aggregate. *Journal of Materials in Civil Engineering*. https://doi.org/10.1061/(ASCE)MT.1943-5533.0000909

Lipczynska, J., West, R. P., Grimes, M., Niall, D., Kinnane, O., & O'Hegarty, R. (2021). Composite behaviour of wide sandwich panels with thin high performance recycled aggregate concrete wythes with fibre reinforced polymer shear connectors. *Journal of Structural Integrity and Maintenance, 6*(3), 187–196. https://doi.org/10.1080/24705314.2021.1906089

Makul, N., Fediuk, R., Amran, M., Zeyad, A. M., de Azevedo, A. R. G., Klyuev, S., Vatin, N., & Karelina, M. (2021). Capacity to develop recycled aggregate concrete in South East Asia. *Buildings, 11*(6), 234. https://doi.org/10.3390/buildings11060234

Mander, J. B., Priestley, M. J., & Park, R. (1988). Theoretical stress-strain model for confined concrete. *Journal of Structural Engineering, 114*(8), 1804–1826. https://doi.org/10.1061/(ASCE)0733-9445(1988)114:8(1804)

Mehta, P., Ezeldin, A., & Aitcin, P.-C. (1991). Effect of coarse aggregate on the behavior of normal and high-strength concretes. *Cement, Concrete, and Aggregates, 13*(2), 121–124. https://doi.org/10.1520/CCA10128J

Mistri, A., Dhami, N., Bhattacharyya, S. K., Barai, S. V., & Mukherjee, A. (2022). Biocement treatment for upcycling construction and demolition wastes as concrete aggregates. *Materials and Structures, 55*(6), 152. https://doi.org/10.1617/s11527-022-01955-3

Nordtest, NT BUILD 492, Concrete, mortar and cement-based repair materials: Chloride migration coefficient from non-steady state migration, Nordtest, Espoo, Finland, 1999.

Ouyang, K., Shi, C., Chu, H., Guo, H., Song, B., Ding, Y., Guan, X., Zhu, J., Zhang, H., Wang, Y., & Zheng, J. (2020). An overview on the efficiency of different pretreatment techniques for recycled concrete aggregate. *Journal Clean Production, 263*, 121264. https://doi.org/10.1016/j.jclepro.2020.121264

Park, S. H., Choi, J. H., Lee, C. Y., Koo, M. S., & Chung, C. W. (2022). Investigation on fire resistance of high-performance cement mortar with recycled fine aggregate mixed by two-stage mixing approach. *Journal of the Korean Recycled Construction Resources Institute., 10*(1), 23–29. https://doi.org/10.14190/JRCR.2022.10.1.23

Poon, C. S., Shui, Z. H., & Lam, L. (2004). Effect of microstructure of ITZ on compressive strength of concrete prepared with recycled aggregates. *Construction and Building Materials, 18*(6), 461–468. https://doi.org/10.1016/j.conbuildmat.2004.03.005

Richard, M. (1984). History of chemical admixtures for concrete. *Concrete International, 6*(4), 40–53.

Ronanki, V. S., & Aaleti, S. (2022). Experimental and analytical investigation of UHPC confined concrete behavior. *Construction and Building Materials, 325*, 126710. https://doi.org/10.1016/j.conbuildmat.2022.126710

Salas, A., Delvasto, S., & Mejía de Gutiérrez, R. (2013). Developing high-performance concrete incorporating highly-reactive rice husk ash. *Ingeniería e Investigación, 33*(2), 9–55. https://doi.org/10.15446/ing.investig.v33n2.39517

Salas-Montoya, A., Chung, C. W., & Mira-Rada, B. E. (2023). Interaction effect of recycled aggregate type, moisture state, and mixing process on the properties of high-performance concretes. *Case Studies in Construction Materials*. https://doi.org/10.1016/j.cscm.2023.e02208

Salas-Montoya, A., & Mira-Rada, B. E. (2023). Evaluation of key aggregate parameters on the properties of ordinary and high strength concretes. *VITRUVIO-International Journal of Architectural Technology and Sustainability, 8*, 76–85. https://doi.org/10.4995/vitruvioijats.2023.19596

Shaban, W. M., Elbaz, K., Yang, J., Thomas, B. S., Shen, X., Li, L., Du, Y., Xie, J., & Li, L. (2021). Effect of pozzolan slurries on recycled aggregate concrete: Mechanical and durability performance. *Construction and Building Materials, 276*, 121940. https://doi.org/10.1016/j.conbuildmat.2020.121940

Shaban, W. M., Yang, J., Su, H., Liu, Q. F., Tsang, D. C., Wang, L., Xie, J., & Li, L. (2019b). Properties of recycled concrete aggregates strengthened by different types of Pozzolan slurry. *Construction and Building Materials, 216*, 632–647. https://doi.org/10.1016/j.conbuildmat.2019.04.231

Shaban, W. M., Yang, J., Su, H., Mo, K. H., Li, L., & Xie, J. (2019a). Quality improvement techniques for recycled concrete aggregate: A review. *Journal of Advanced Concrete Technology, 17*(4), 151–167. https://doi.org/10.3151/jact.17.151

Silva, R. V., de Brito, J., & Dhir, R. K. (2018). Fresh-state performance of recycled aggregate concrete: A review. *Construction and Building Materials, 178*, 19–31. https://doi.org/10.1016/j.conbuildmat.2018.05.149

Singh, A., Duan, Z., Xiao, J., & Liu, Q. (2020). Incorporating recycled aggregates in self-compacting concrete: A review. *Journal of Sustainable Cement-Based Materials, 9*(3), 165–189. https://doi.org/10.1080/21650373.2019.1706205

Tam, V.W.-Y., Gao, X.-F., & Tam, C. M. (2006). Comparing performance of modified two-stage mixing approach for producing recycled aggregate concrete. *Magaz. Concr. Res., 58*(7), 477–484. https://doi.org/10.1680/macr.2006.58.7.477

Tam, V. W. Y., Soomro, M., & Evangelista, A. C. J. (2018). A review of recycled aggregate in concrete applications (2000–2017). *Construction and Building Materials, 172*, 272–292. https://doi.org/10.1016/j.conbuildmat.2018.03.240

Tam, V. W. Y., & Tam, C. M. (2007). Assessment of durability of recycled aggregate concrete produced by two-stage mixing approach. *Journal of Materials Science, 42*, 3592–3602. https://doi.org/10.1007/s10853-006-0379-y

Tam, V. W. Y., & Tam, C. M. (2008). Diversifying two-stage mixing approach (TSMA) for recycled aggregate concrete: TSMAs and TSMAsc. *Construction and Building Materials, 22*(10), 2068–2077. https://doi.org/10.1016/j.conbuildmat.2007.07.024

Tam, V. W., Wattage, H., Le, K. N., Butera, A., & Soomro, M. (2023). Hybrid methods to improve microstructure of recycled concrete and brick aggregate for high-grade concrete production. *Magazine of Concrete Research, 75*(1), 17–31. https://doi.org/10.1680/jmacr.21.00233

Tam, V. W. Y., Wattage, H., Le, K. N., Buteraa, A., & Soomro, M. (2021). Methods to improve microstructural properties of recycled concrete aggregate: A critical review. *Construction and Building Materials, 270*, 121490. https://doi.org/10.1016/j.conbuildmat.2020.121490

Wu, W. (2019). Advanced composite structure combining Ultra high performance concrete with normal reinforced concrete. *MATEC Web of Conferences, 278*, 03004. https://doi.org/10.1051/matecconf/201927803004

Xuan, D., Zhan, B., & Poon, C. S. (2016). Assessment of mechanical properties of concrete incorporating carbonated recycled concrete aggregates. *Cement and Concrete Composites, 65*, 67–74. https://doi.org/10.1016/j.cemconcomp.2015.10.018

Yehia, S., Helal, K., Abusharkh, A., Zaher, A., & Istaitiyeh, H. (2015). Strength and durability evaluation of recycled aggregate concrete. *International Journal of Concrete Structures and Materials, 9*(2), 219–239. https://doi.org/10.1007/s40069-015-0100-0

Zhang, H., Ji, T., Liu, H., & Su, S. (2018). Modifying recycled aggregate concrete by aggregate surface treatment using sulphoaluminate cement and basalt powder. *Construction and Building Materials, 192*, 526–537. https://doi.org/10.1016/j.conbuildmat.2018.10.160

Zheng, Y., Zhang, Y., & Zhang, P. (2021). Methods for improving the durability of recycled aggregate concrete: A review. *Journal of Materials Research and Technology, 15*, 6367–6386. https://doi.org/10.1016/j.jmrt.2021.11.085

Publisher's Note

Ji-Hyun Kim is an Assistant Professor at Pukyong National University, South Korea. She obtained her B.E. (2005), M.E. (2007) and Ph.D. (2010) in Architectural Engineering, Pukyong National University. She worked as a Research Professor at Multidisciplinary Infra-technology Research Laboratory during September 2016 to August 2024 and joined the Division of Architectural and Fire Protection Engineering as an Assistant Professor. Her research interest is in the utilization of industrial by-products and recycled aggregates, and high-durability concrete using nanomaterials.

Andrés Salas-Montoya is an Associate Professor in the Department of Civil Engineering at the Universidad Nacional de Colombia in Manizales, Colombia. He obtained his Ph.D. in Materials Engineering and completed a post-doctoral appointment in Civil and Environmental Engineering at the University of Illinois at Urbana-Champaign, USA. With over 30 years of experience, Dr. Salas-Montoya specializes in sustainable construction, focusing on low-carbon materials, waste-based building materials, natural fibers, and pozzolanic composites. He has held key administrative roles, significantly contributing to international collaborations in sustainable engineering education and research.

Young-Chan Kim is an Emeritus Professor in the Division of Architectural and Fire Protection Engineering at Pukyong National University, South Korea. He obtained his B.E. (1983) and M.E. (1985) in Architectural Engineering, Seoul National University, and his Ph.D. (1995) in Civil and Environmental Engineering, West Virginia University. Before he joined Pukyong National University at 1998, he had worked as a Research Manager at Daelim E&C, for 1995–1997. His specialty is in the area of structural engineering.

Chul-Woo Chung is a professor and chair in the Division of Architectural and Fire Protection Engineering at Pukyong National University, South Korea. He obtained his B.E. (1998) and M.E. (2000) in Architectural Engineering, Pusan National University, and his M.S. (2004) and Ph.D. (2010) in Civil and Environmental Engineering, University of Illinois at Urbana-Champaign. Before he joined Pukyong National University at 2012, he had worked as a cement chemist/scientist at Pacific Northwest National Laboratory, USA, for 2010~2012. His specialty is in the area of cement-based materials with a focus on sustainable and advanced cementitious materials.